
# Use SNA instead of VNA to characterize indoor channel

Name: Liu Che

Lai Jingou

Examiner : José Chilo

# Abstract

In this report we focus on the use of an economical way on how Scalar Network Analyzer (SNA) works instead of Vector Network Analyzer (VNA) to estimate the phase angle of signals in indoor channel. This is detailed in RMS delay theory and simulation section, experimental is designed in the according Experiment Design section, where we also state the required measurements known from the math part. In our work, data are recorded both from two different channel characteristics. Method of achieving amplitude is by using deconvolution theory. The condition of applying Hilbert transform are highlighted as impulse response h(t) in time domain should be causal. The recorded data amplitude is computed by Hilbert Transform, and therefore validate the condition using Inverse Discrete Fourier Transform (IDFT) back to time domain to achieve h(t). Power delay profile P(t) is therefore presented afterwards. In paper calculations of rms delay $\tau_{rms}$ of the channel which is the most important variable are also performed, the results calculated from different windowing truncation and the LOS and NLOS characteristics are compared in discussion and conclusion section, it also includes Opinions of window functions chosen for the phase estimation.

# Contents

# 1. Introduction

VNA has taken place of SNA for decades, for better functionalities, VNA has the function to measure signal phase information in Frequency domain, which function SNA does not have[1], But VNAs are expensive, and the requirement of low-loss, high price long RF cable are becoming one of the most important economical motivations to do this work[2].

For the channel impulse response, usually we use pulse generator and digital oscilloscope to measure in time domain in a directly way[3,4] , but we can also use Network Analyzer in an indirect way through inverse transform from frequency domain to time domain, therefore we need the complex vector or amplitude and phase angle.

The question would be raised; can we use SNA to do this measurement? Since we know SNA can only measure amplitude, but not the phase angle. In our work, the way on how to measure radio signal phase information using SNA is presented, the method is based on Hilbert transform relationship between the real and imaginary part of the spectrum of the analytic signal [5], and therefore the phase of the signal can be recovered.

To estimate characteristics of the channel, RMS delay is the most important variable to know. And to know RMS delay, mean delay is the condition; power delay profile information of that signal must be gained to calculate mean delay value which value we cannot tell before impulse response is known; the steps of calculation RMS delay will also reveal the order. As the result, the objectives of this paper: channel impulse response and rms are therefore calculated from existed assumption [5,6]. It is calculated from measurements in frequency domain using SNA.

For frequency domain measurement, modulated signal generated by a synthesizer is recorded by a SNA instead of VNA. Antennas, receiver with amplification and synchronization are presented in the followed radio system [2].

Since SNA only can measure spectrum information, the phase is estimated by applying the Hilbert transform on the logarithm (base on mathematical constant e) over the spectrum of that signal [5]. The condition of calculation above is H(jω) has minimum phase, another word, all the zeros of transfer function H(jω) lies in the left plane of complex s domain[5].

The phase of H (jw), together with spectrum of H(jw), Inverse Discrete Fourier Transform can be therefore applied on them to retrieve impulse response h(t). h(t) can be employed to calculate power delay profile(PDP), therefore mean delay and rms delay can be obtained[6]. Then the goal is reached by getting rms delay.

To get transfer function spectrum, we apply deconvolution theory, division from the spectrum of Y (jw) and spectrum of X(jw)

Structures of the report are:

*RMS delay theory and simulation* section highlights the mathematical explanation of the work in order to be understood. We take an example to illustrate how RMS delay can be calculated in steps.

In the *experiment design* section it illustrates the ways to measure in order to achieve signals in math section as well as present the construction of a system required to our work, there are two type of system light of sight (LOS) and none light of sight(NLOS).

In *discussion and result*, we summary our work, also compare the appearance of different window functions on the same measurements, the window function we are chosen to truncate the results are from the high resolution to the low resolution, each of them is on every result, therefore comparison can be made. We make the comparison of Los system and NLOS system variables (Impulse response, RMS delay) in different group of windows.

# 2. RMS Delay Theory and Simulations

To understand this report we need some theories. First of all, most importantly, Root-mean-square (RMS) delay spread is associated with the power lines, it is important information for determining the data transmission rate. The maximum transmission rate is the inverse proportional to RMS delay [7].

Convolution in time domain is equivalent to multiplication in frequency domain, which is [8]:

$$|Y(j\omega)| = |X(j\omega)| \bullet |H(j\omega)| \tag{1}$$

The recorded wire and wireless channel measured in next section by SNA, Y(jω), X(jω) are using division to accomplish the deconvolution theory, for the division in Frequency domain is equivalent to deconvolution, in time domain[7]:

$$|H(j\omega)| = |Y(j\omega)| / |X(j\omega)| \tag{2}$$

In which Y (jω), X (jω), H (jω) are in frequency domain. H(jω) will result as the transfer function of the channel in frequency domain.

For narrow band signal modulated wire channel spectrum X(jω) is in figure1.1, wireless response Y(jω) is in figure1.2

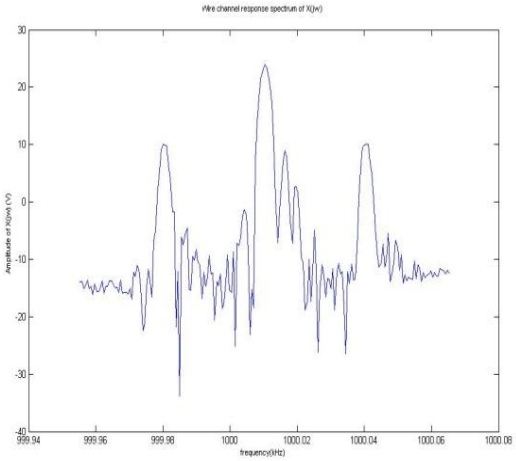

Figure 1.1 X(jω)

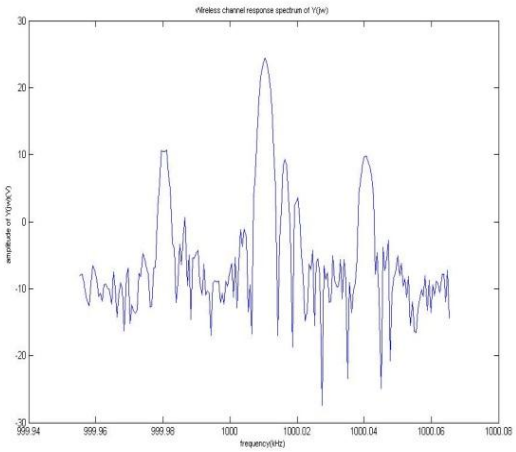

Figure 1.2 Y(jω)

Here are 5 steps presented below to calculate RMS delay profile:

*Step 1 Truncate the Transfer Function Spectrum with different window functions:*

It has been illustrated that the phase retrieval works better with hanning window than rectangular due to its lower side lobe level.[9] In the work we truncate with 4 type of window: rectangular presented in figure1.3, Blackman-Harris in figure1.4, Hanning window in figure 1.5, Kaiser (β = 2) in figure 1.6. we employ Blackman-Harris as a lower side lobe window than hanning.

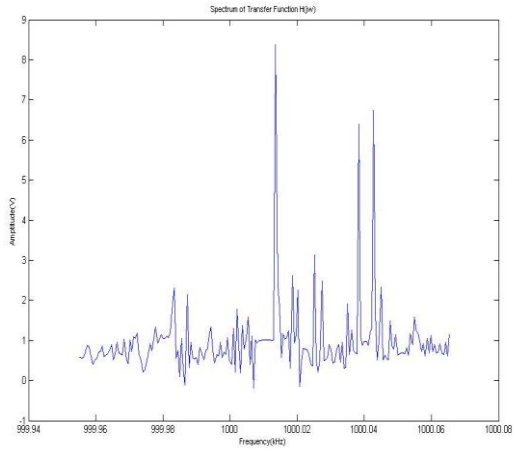

Figure 1.3 Spectrum with rectangular window

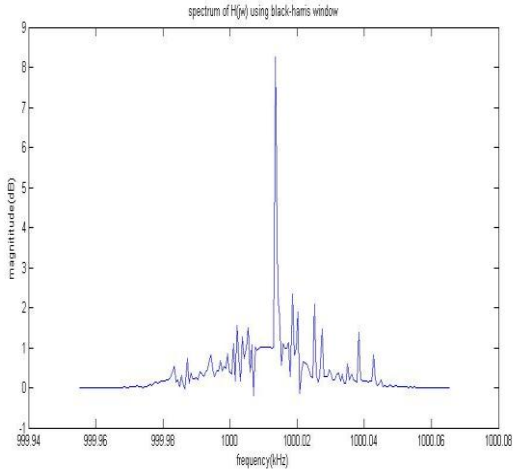

Figure 1.4 Spectrum with Blackman-Harris window

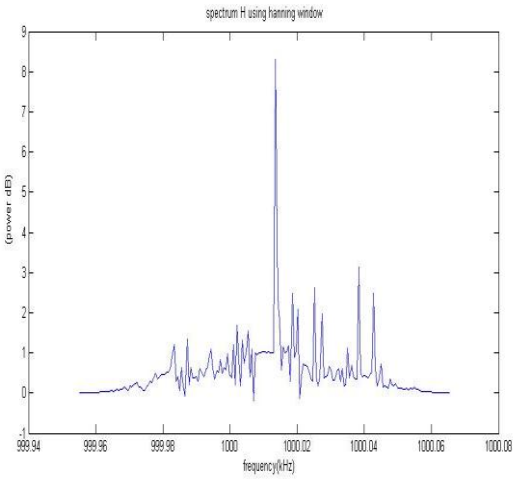


Figure 1.5 Spectrum with hanning window

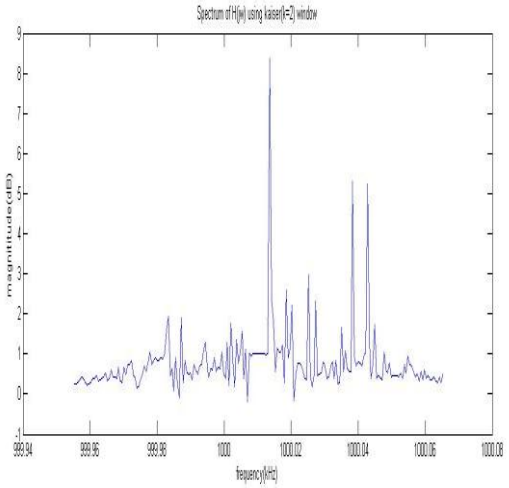


Figure 1.6 Spectrum with Kaiser window (β = 2)

On matlab, the commands have been added in appendix C, windowing truncation.

*Step 2: Make phase angle estimation:*

H(jw) is normally constituted of real part $H_R$(jw) and imaginary part $H_I$(jw) [5]:

$$H(j\omega) = H_R(j\omega) + jH_I(j\omega) \tag{3}$$

$$= H_R(j\omega) + j\Psi[H_R(j\omega)] \tag{4}$$

The spectrum phase information is calculated through the spectrum using formular [5]:

$$\arg H(j\omega) = \Psi[\log|H(j\omega)|] = \theta \tag{5}$$

Operation $\Psi$ [.] operator denoted as Discrete Hilbert Transform, log [.] operator denoted as logarithm based on constant e. If h(t) is causal , the phase of H(jw) is then illustrated below[5], we both illustrate the phase angle truncated with different windows: rectangular window presented in figure1.7, Blackman-Harris window in figure1.8, Hanning window in figure 1.9, Kaiser(β = 2) window in figure 1.10.

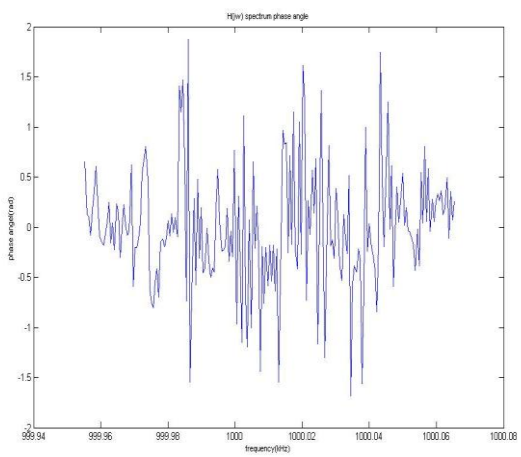


Figure 1.7 Phase estimation using rectangular window

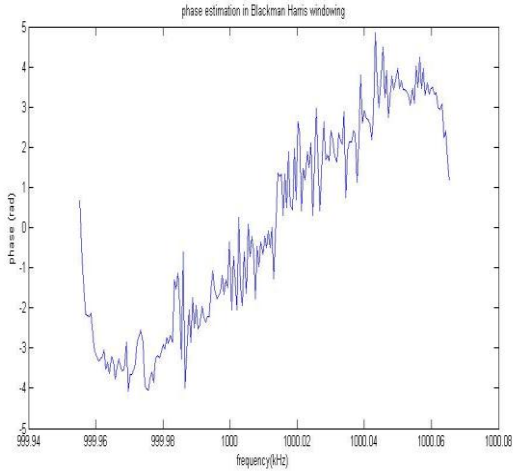


Figure 1.8 Phase estimation in Blackman Harris window function

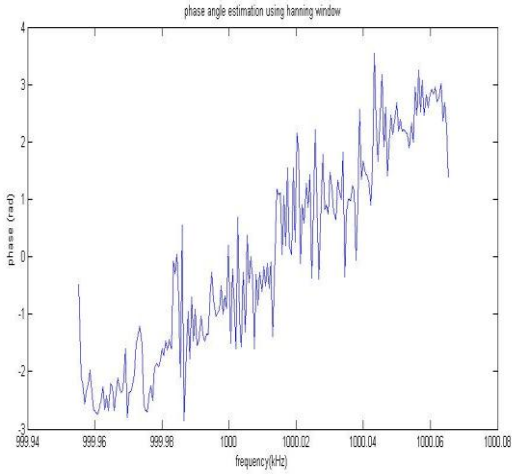


Figure 1.9 Phase estimation in hanning window function

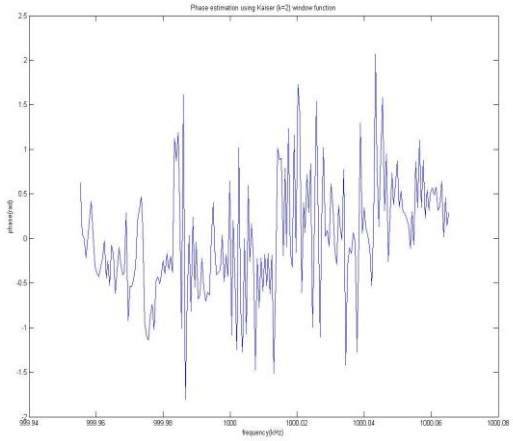


Figure 1.10 Phase estimation in Kaiser Beta2 window function

For commands in matlab, see appendix C, phase angle.

*Step 3, apply inverse fourier transform (ifft) to achieve impulse response h(t):*

Amplitude together with the phase of the spectrum, the signal could be written in (6).

$$Ae^{j\theta} = A(i*\sin\theta + \cos\theta) \tag{6}$$

Now we can use in the Inverse fast Fourier Transform IFFT. The impulse response will be achieve in discrete data because both X(jω), Y(jω) are discrete in points, so h(n) could be reached by applying Inverse Discrete Fourier Transform[10]:

$$x(n) = \frac{1}{N}\sum_{k=0}^{N-1} X(\frac{2\pi}{N}k)e^{j2\pi kn/N}, 0 \le n \le N-1 \quad (7)$$

For the formula in our simulation, n=0,1,2,3,4…..N-1, k=0,1,2,3,4…..N-1 and N=201. The unit transfer from frequency (Hz) unit to time unit (second). For one sample point on frequency domain, the time resolution is 1/fs, which sampling frequency fs is calculated as:

fs= $\Delta f*(N_{points}-1)$[11], which is about 9 μs in example above. So in the x axis the time domain is from 0 to (201-1)* 9 μs in 201 point increased in 9 μs in each successive points. After applied inverse fourier transform to H(jω), which we have a complex value, the result would be impulse response, which is in time domain, can fully describe the channel characteristic

Form figure 1.11 to 1.14 show the impulse response truncated in different window functions: rectangular window presented in figure1.11, Blackman-Harris window in figure1.12, Hanning window in figure 1.13, Kaiser (β = 2) window in figure 1.14.

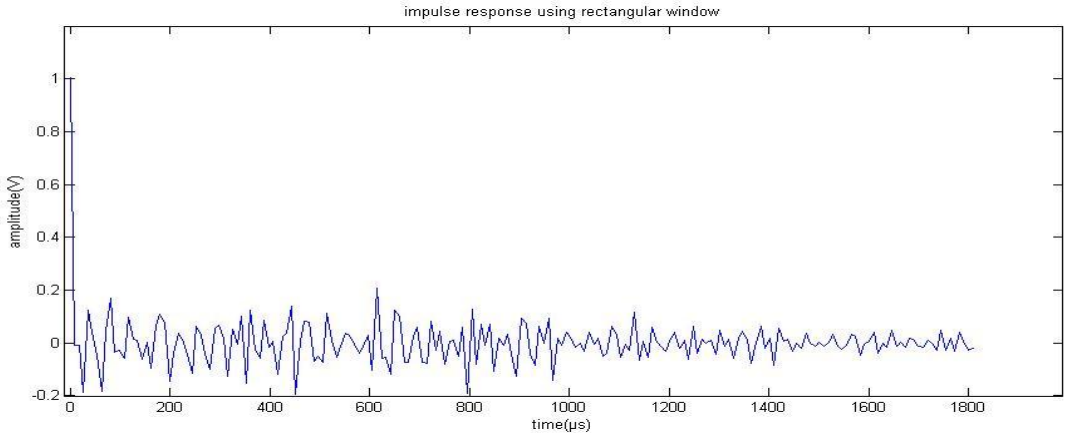


Figure 1.11 Impulse response from rectangular window

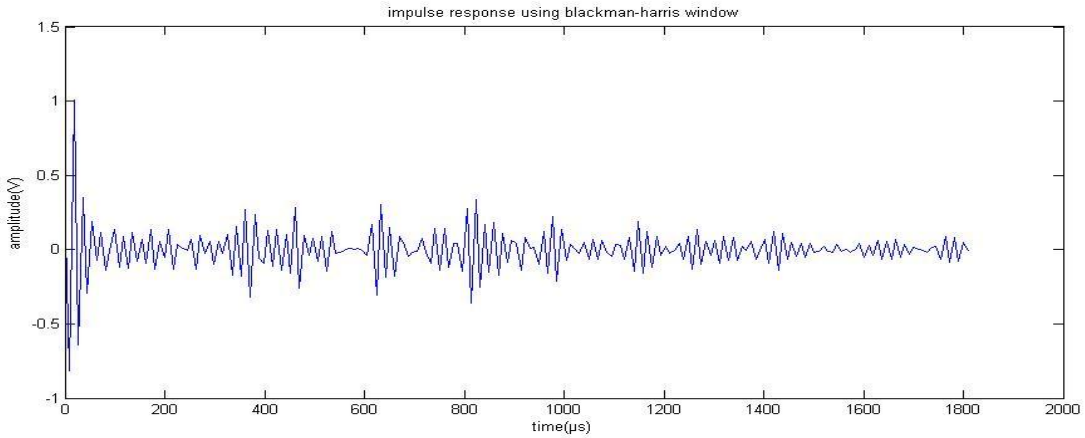


Figure 1.12 impulse response from blackman-harris window

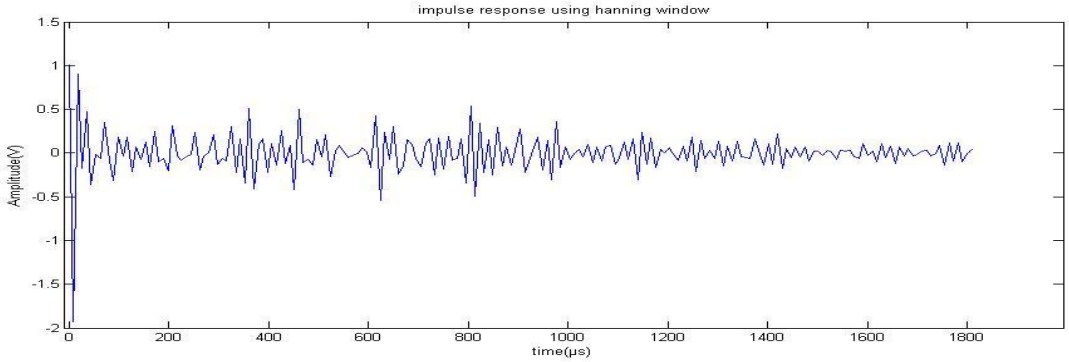


Figure 1.13 Impulse response from hanning window

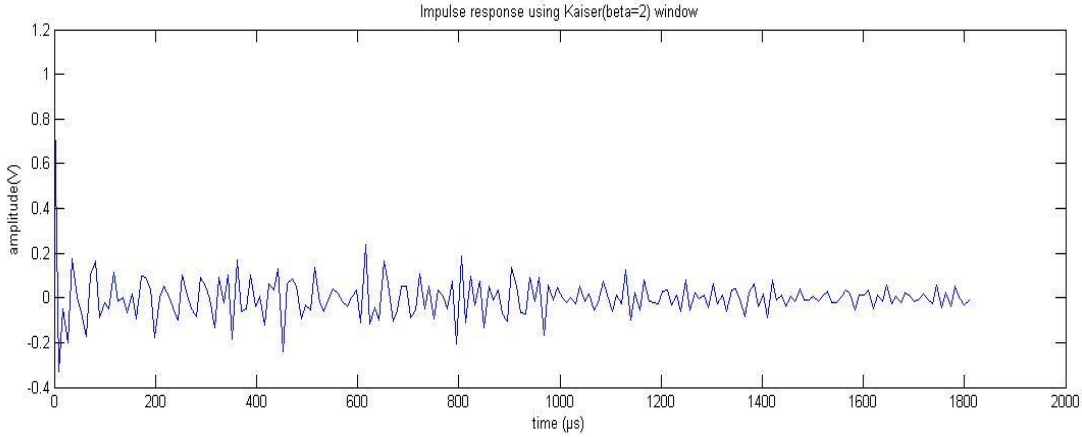


Figure 1.14 Impulse response from Kaiser window

Commands for retrieve impulse response see Appendix C, impulse response.

*Step 4 estimate power delay profile from impulse response:*

In the study, the impulse response of an AC power line S(n) is assumed to have a finite duration N. As the square of impulse response is equal to the power delay profile (PDP), which is simply [6]:

$$P(t) = |h(t)|^2 = \sum \alpha^2{}_k \delta(\tau - \tau_k) \tag{8}$$

Figure 1.15 to figure 1.18 shows the power delay profile with windows rectangular, Blackman-Harris, Hanning, Kaiser (Beta=2), respectively.

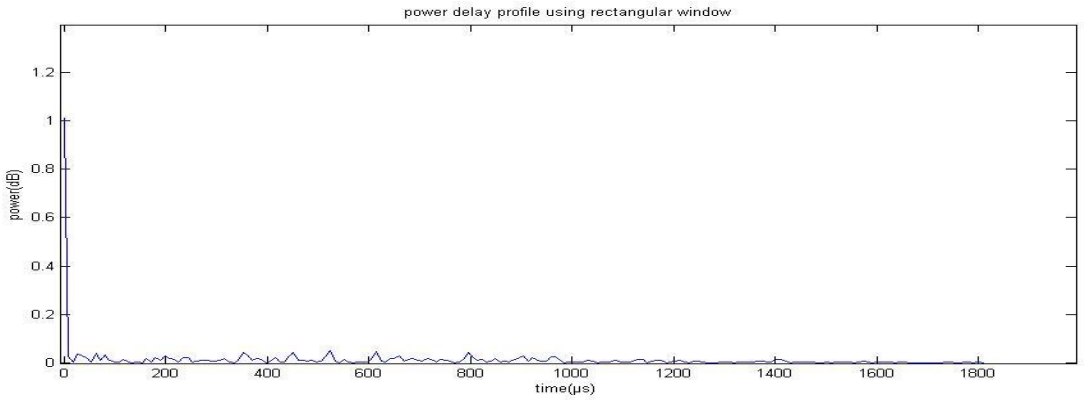


Figure 1.15 Power delay profile using rectangular window

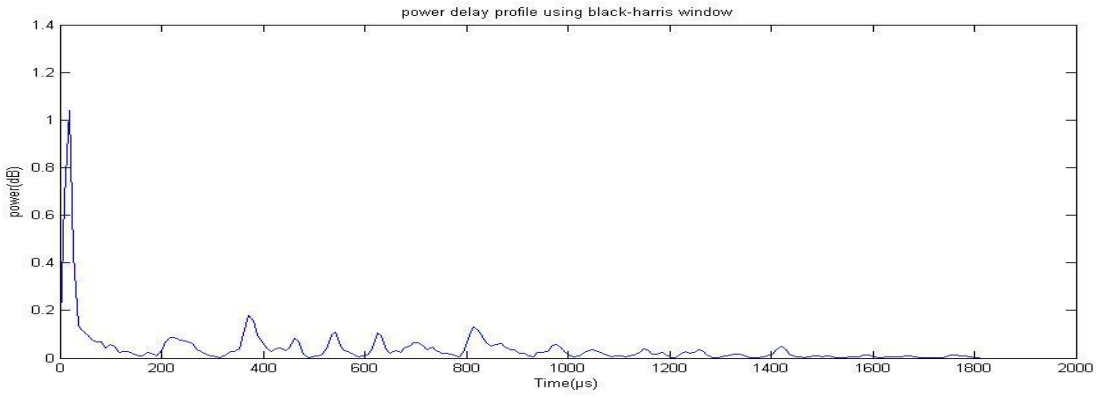


Figure 1.16 power delay profile using blackman harris window

The results of different window power delay profile (PDP) are also presented in figure: one can easily see the differences.

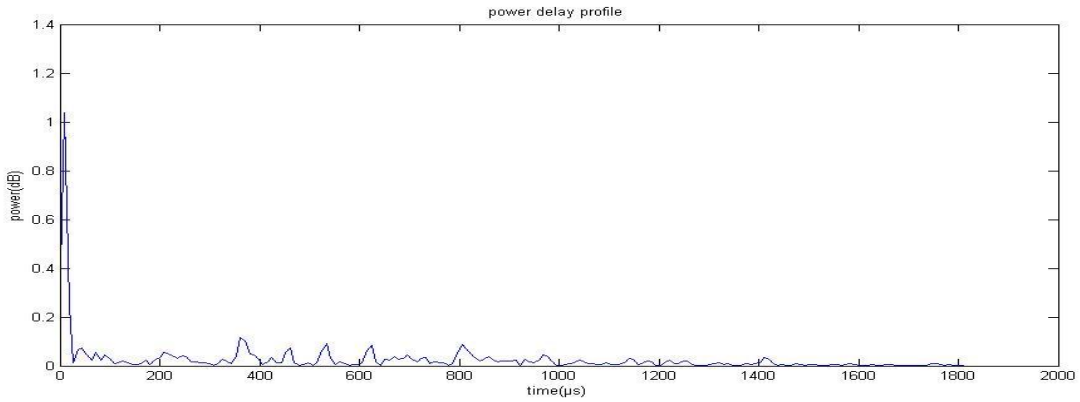


Figure 1.17 power delay profile using hanning window

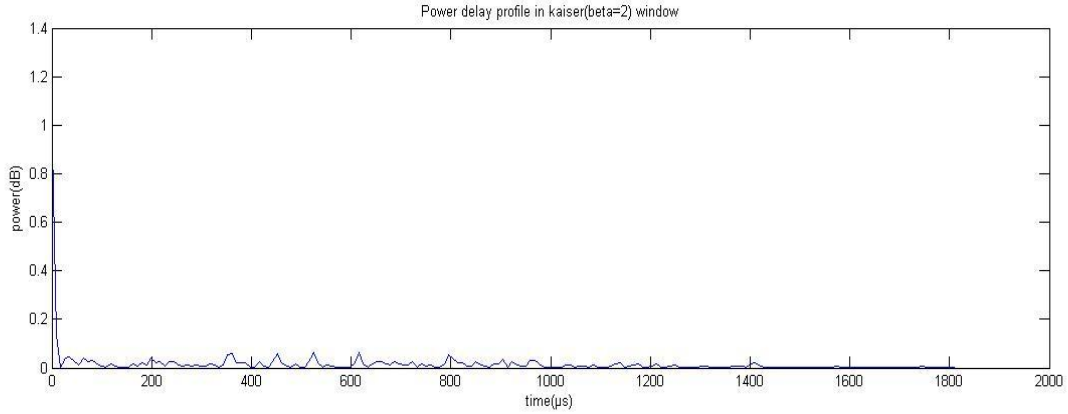


Figure 1.18 Power delay profile using Kaiser (β=2) window

Commands in matlab are included in Appendix C, power delay profile.

Step 5, Calculation of the mean delay μ and rms delay $\tau_{rms}$[7]:

$$u = \frac{\sum_{n=1}^{M} nP(t)}{\sum_{n=1}^{M} P(t)} \quad (9)$$

and after, RMS delay can be calculated as[7]:

$$\sigma_{RMS} = \sqrt{\frac{\sum_{n=1}^{M}(n-u)^2 P(t)}{\sum_{n=1}^{M} P(t)}} \quad (10)$$

Where n is point number from 1 to 201, u is mean delay, P(t) is power delay profile.

The comparison between the window functions is shown below:

| Propagation in light of sight (LOS) | | | | |
|---|---|---|---|---|
| | Rectangular | Blackman Harris | Hanning | Kaiser(β=2) |
| Mean delay(μs) | 43.41 | 52.23 | 50.27 | 46.58 |
| RMS delay (μs) | 48.91 | 49.08 | 49.319 | 49.33 |

Table 1

Commands to calculate mean delay and rms delay are mentioned in Appendix C, mean delay and RMS delay.

# 3. Experiment Design

## 3.1 Experiment Principle

First, we connect Synthesizer and SNA with coaxial wire [12] and measure the signal response between Synthesizer, coaxial cable, and SNA, that is frequency response X(jω). Second, Y(jω) is the measurement using the same coaxial cable connected with antenna and synthesizer or SNA, Y(jω) is the frequency response of Synthesizer, coaxial cable, radio channel and SNA. Deconvolution is done by using the equation (1), which result will come out H(jω).

Then a ifft method is applied on H(jω), which H(jω) will transfer from frequency domain back to time domain, namely it is h(t), but before H(jω) need to have phase angel, that is where the Hilbert transform should be applied, in formula(3), Argument of H(jω) is easily computed. Formula (6) is the the finally transformation before we achieve h(t).

Power delay profile (PDP) is the square of the absolute value of h(t). Then mean delay μ is calculate via (8), rms delay σ is therefore achieved by perform (9), that's the specified rms delay of distance between 2 antennas.

The signal used to do transmission:  AM signal with carrier: 2.45GHz, and Intelligent signal (information) is 30 kHz Square wave signal with $V_{pp}$ 5 V.

Use SNA to measure signal in frequency domain, 11.2dBm power amplifier is include in Rake receiver, 2 dipole antennas are employed for transmission and reception

The frequency of interest On SNA are:  Center frequency is 2.45GHz, the span is 500 MHz, the estimated signal achieved from SNA is the signal power concentrate on the center frequency 2.45GHz, and less but also concentrate on the several frequencies. The signal in frequency domain is recorded in 1601 points, therefore 0.3125MHz rise up for each point. In the time domain the resolution is $1/f_{sampling}$ which is 1/ (Δf*N-1) [11] and equal to 1.99ns

To achieve H (jω) we need to do measurements wired test and wireless test:

## 3.2 Wired Test

Figure 2.1 shows the experiment setup used for the wired test, in which experiment we can measure amplitude response $|X(j\omega)|$.

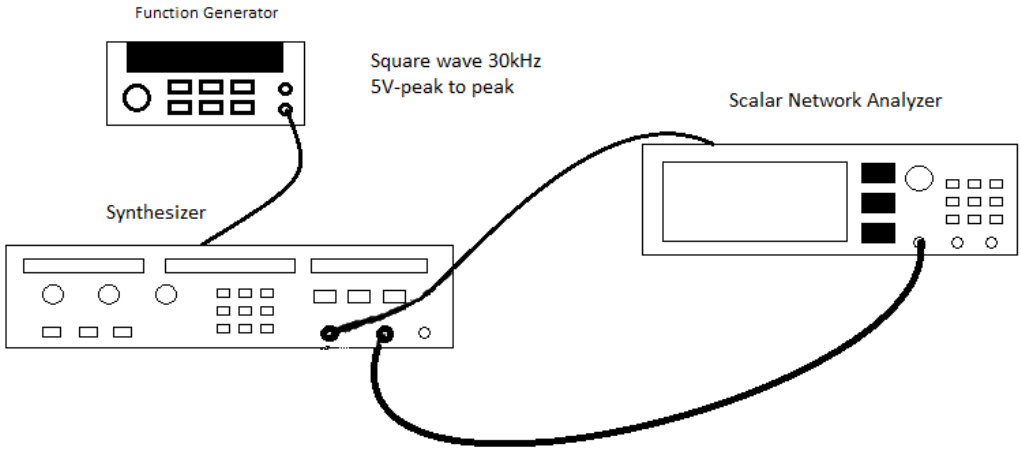


Figure 2.1 connection of wired test

Function generator is connected to the External port of Synthesizer. And the RF output of Synthesizer connects to the Scalar Network Analyzer directly.

Intelligence signal is square wave with frequency 30 kHz, $5V_{pp}$. Carrier signal is 2450MHz sine wave. The type of the modulation is amplitude modulation (AM). The AM depth is 30%, the power level is 11.2dBm on the Synthesizer (Signal Generator Marconi Instruments 2031).

For the experiment instruments, we use Function generator (HP33120A), Synthesizer and Scalar Network Analyzer.

The amplitude response shows the signal from 2.2GHz to 2.7GHz. For such wide band, the square wave in modulated signal can be nearly stored completely.

## 3.3 Wireless Test

Then for wireless test which is shown on Figure 2.2, in which experiment we measure amplitude response $|Y(j\omega)|$.

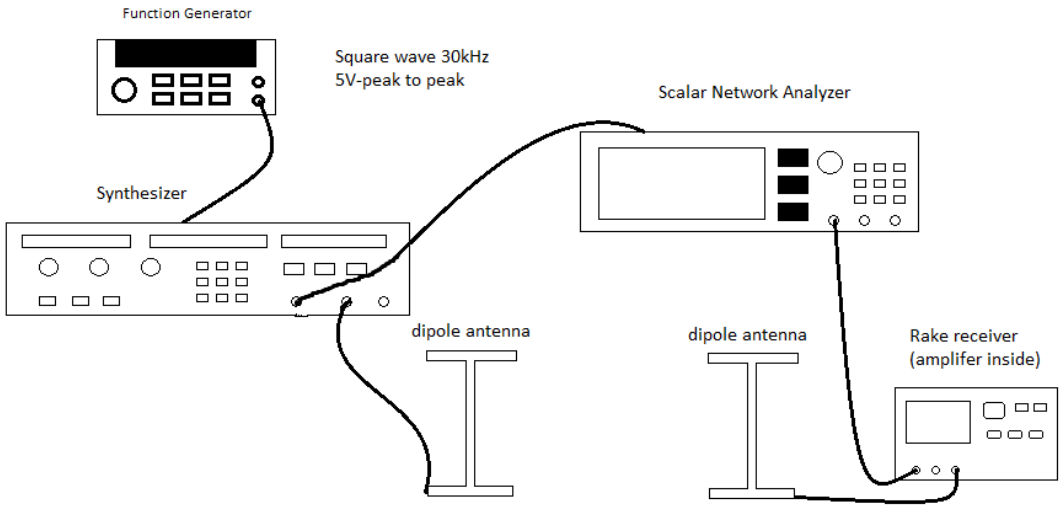


Figure 2.2 connection of wireless test

Function generator connects to the External port of Synthesizer. The cable between transmitting and receiving is connecting sweep out port of synthesizer to the Scalar Network Analyzer. The RF-output connect the transmitting antenna which on the desk and separate the receiving antenna approximately 16m using line of sight propagation. The receiving antenna connects to the input port of rake receiver [13]. The output of rake receiver connects to Scalar Network Analyzer.

Intelligence signal is square wave with frequency 30 kHz, $5V_{pp}$. Carrier signal is 2450MHz sine wave. The type of the modulation is amplitude modulation (AM). The AM depth is 30%,

the power level is 11.2dBm on the Synthesizer. The sweep signal is 1Hz saw-tooth signal. The type of Instruments used: Function generator (HP33120A), Synthesizer (Signal Generator Marconi Instruments 2031), Rake receiver and Antennas (dipole antenna), Scalar Network Analyzer.

All the instruments information are included in appendix A.

Figure 2.3 and 2.4 show the amplitude response $|X(j\omega)|$ and $|Y(j\omega)|$, respectively. The Span is 0.5GHz, center frequency is 2450MHz.

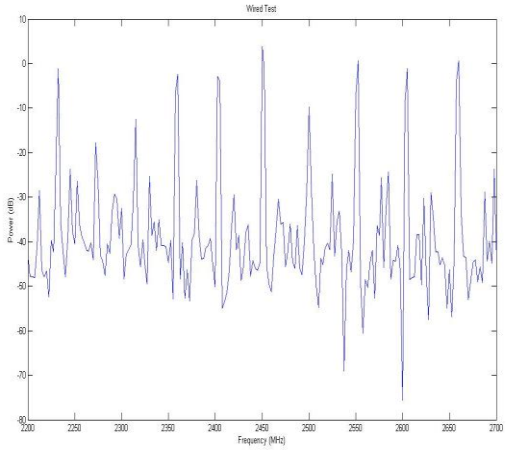


Figure 2.3 spectrum for wired test

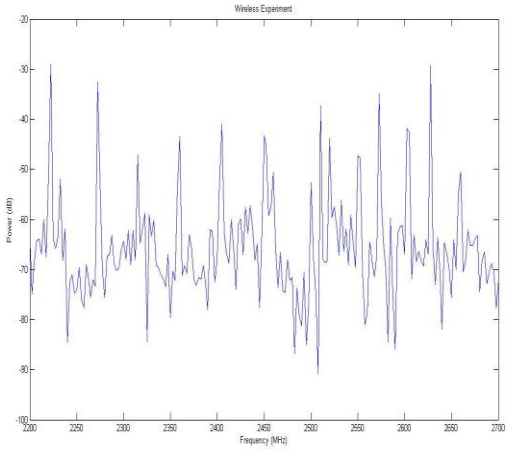


Figure 2.4 spectrum for wireless test

The spectrum is similar to wired in order to apply the deconvolution method.

# 4. Processing and Results

## *4.1 Processing of Line of sight propagation (LOS) results*

*Step1 frequency spectrum result truncated with different window functions*

Apply the deconvolution method which based on $|H(j\omega)| = |Y(j\omega)| / |X(j\omega)|$ to get the frequency spectrum in rectangular window, Kaiser $(\beta = 16)$ Window, which in contrast of kaiser $(\beta = 2)$ in illustration, and hanning window, Blackman-Harris window.

As the Rectangular window w(n)=1, it keeps the frequency spectrum constant. However it has the thinnest main lobe compare with Kaiser Beta16 Window, Hanning Window and Blackman-Harris window.

Hanning Window has wider main lobe than rectangular window and thinner main lobe than Blackman-Harris window, Kaiser Beta16 Window.

Compare with rectangular window and hanning window, the expression of the Blackman-Harris is more complicated. It minimizes side-lobe levels. However, the main lobe is the wider than Hanning and Rectangular Window.

So the widths of window functions are:

Kaiser Beta16 > Blackman-Harris > Hanning > Rectangular

Form figure 3.1 to 3.4 show the frequency spectrum truncated in different window functions: Rectangular window presented in figure3.1, Kaiser (β = 16) window in figure3.2, Hanning window in figure 3.3, Blackman-Harris window in figure 3.4.

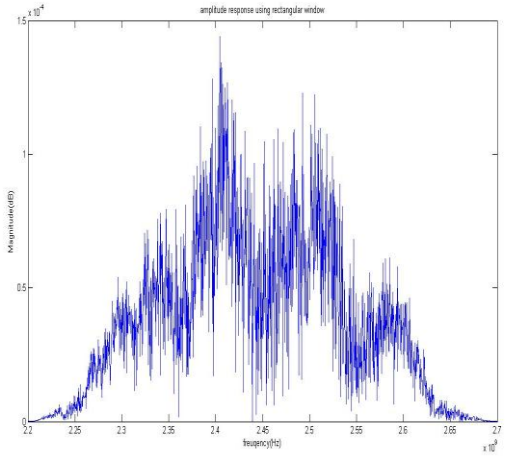


Figure 3.1 LOS frequency spectrum using rectangular window

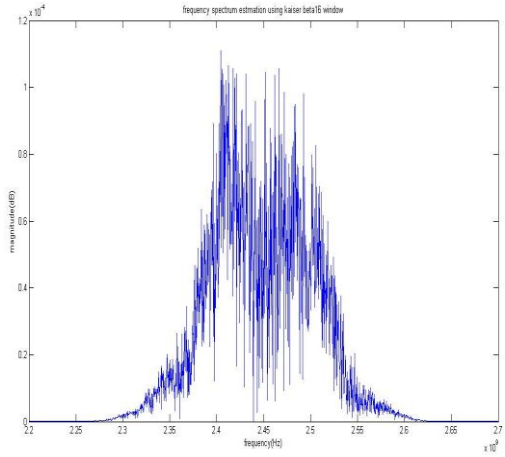


Figure 3.2 LOS frequency spectrum using kaiser beta16 window

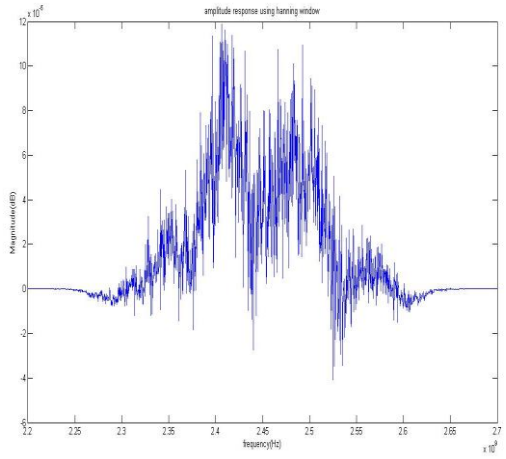


Figure 3.3 LOS frequency spectrum using hanning window

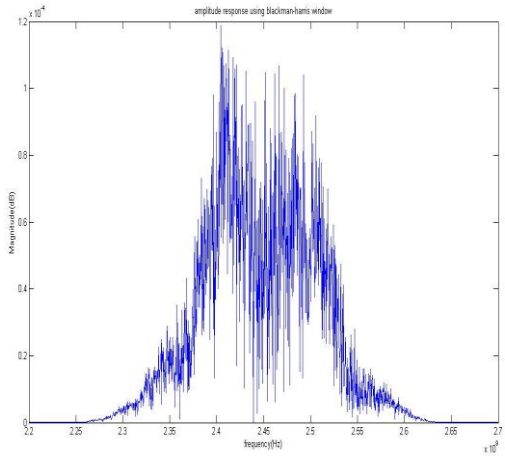


Figure 3.4 LOS frequency spectrum using blackman-harris window

*Step2 Compute the phase angle*

Process the Hilbert transform on the logarithm of frequency spectrum to create the imaginary part of $\log|H(j\omega)|$ ------the phase angle, which is equation of (5).

The phase angles truncated in different window functions are shown below:

Rectangular window presented in figure3.5, Kaiser (β = 16) window in figure3.6, Hanning window in figure 3.7, Blackman-Harris window in figure 3.8.

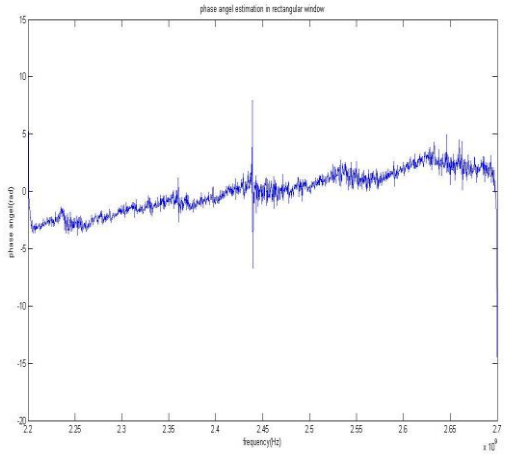


Figure 3.5 LOS phase angle estimation using rectangular window

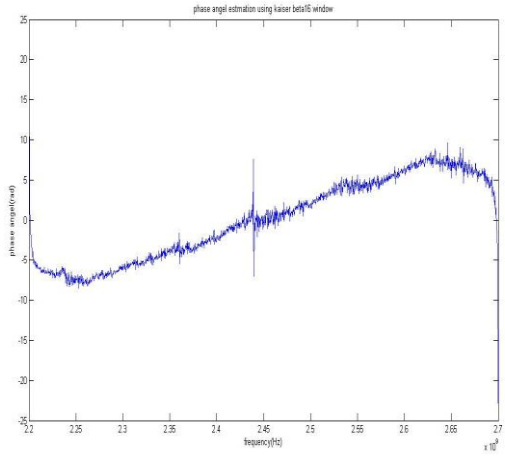


Figure 3.6 LOS phase angle estimation using kaiser beta16 window

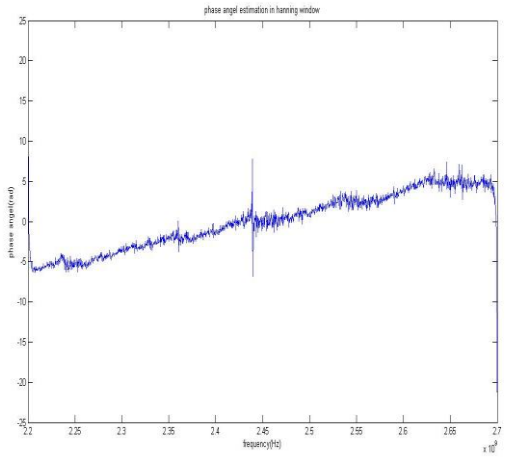


Figure 3.7 LOS phase angle using hanning window

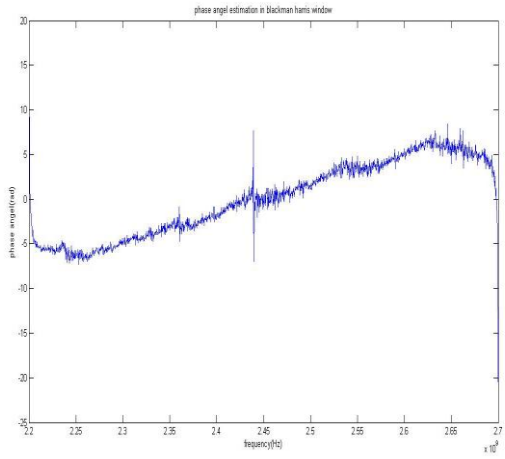


Figure 3.8 LOS phase angle using blackman-harris window

*Step3 Calculate the impulse response*

As illustrated, in formula (6), $H(j\omega)$ stands for complex signal,

Phase estimation together amplitude, the inverse fast Fourier transform is applied to transfer the complex signal from frequency domain to time domain and get the impulse response h(t) and truncated in different window functions. For time domain resolution, $1/f_s$, that is about 1.99ns, and time axis is from 0 to 3198ns.

The impulse response truncated in different window functions are shown below:

Rectangular window presented in figure3.9, Kaiser (β = 16) window in figure3.10, Hanning window in figure 3.11, Blackman-Harris window in figure 3.12

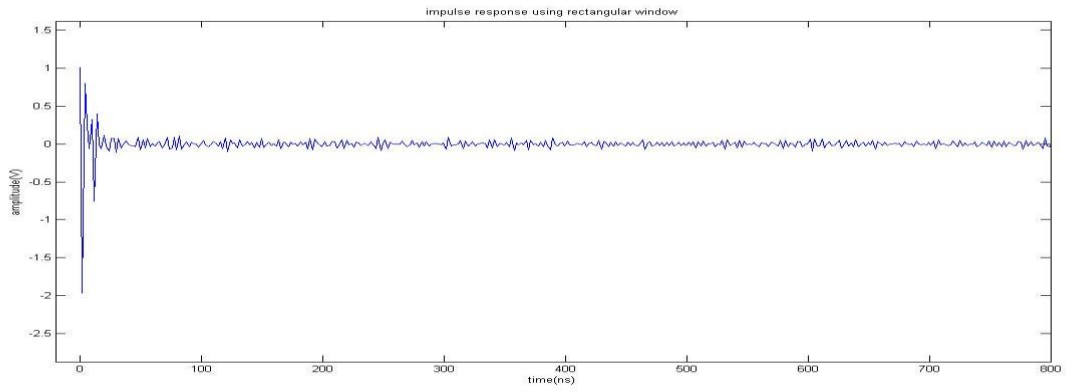


Figure 3.9 LOS impulse response using rectangular window

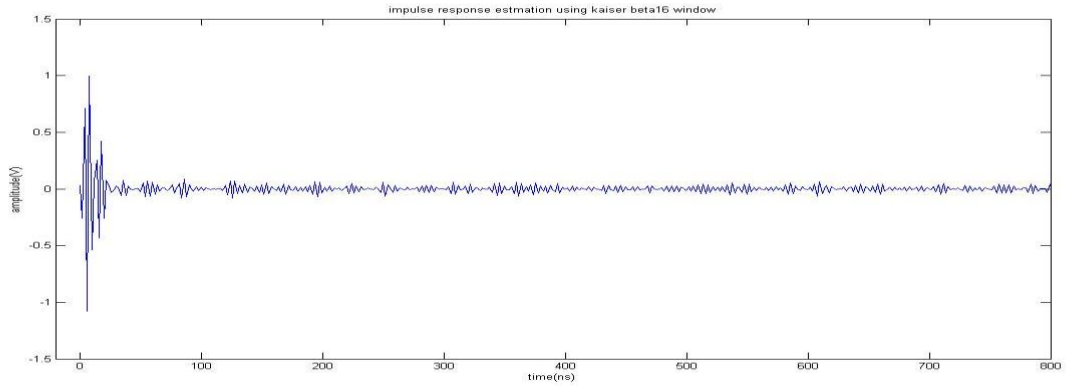


Figure 3.10 LOS impulse response using Kaiser beta16 window

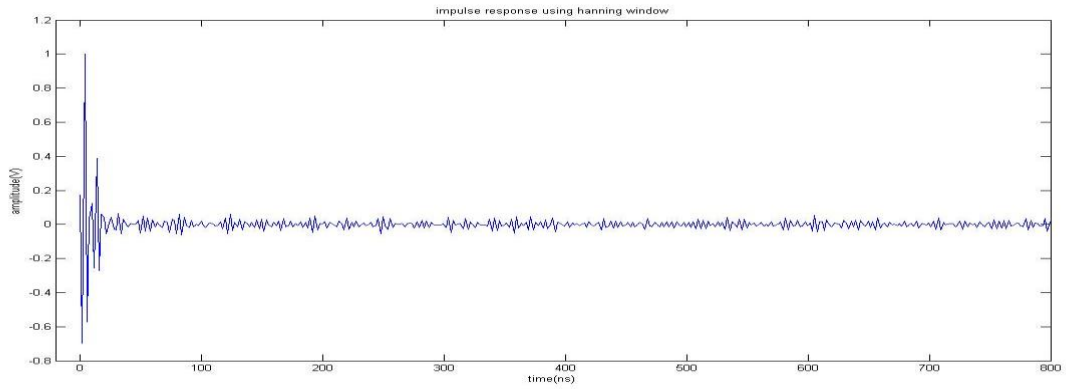


Figure 3.11 LOS impulse response using hanning window

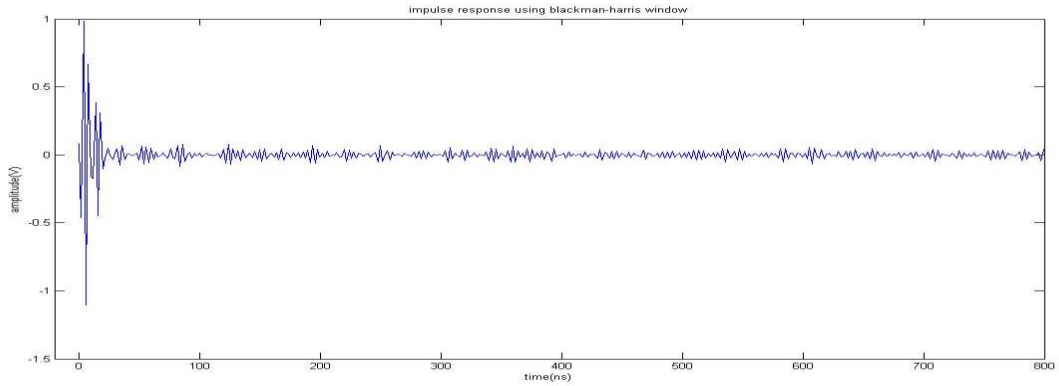


Figure 3.12 LOS impulse response using blackman-harris window

*Step4 Find out the Power Delay Profile*

The Power Delay Profile (PDP) is equal to the square of absolute value for impulse response, $P(t) = |h(t)|^2$ ,illustrated in formula(8).

The Power Delay Profile truncated in different window functions are shown below:

Rectangular window is presented in figure3.13, Kaiser (β = 16) window in figure3.14, Hanning window in figure 3.15, Blackman-Harris window in figure 3.16:

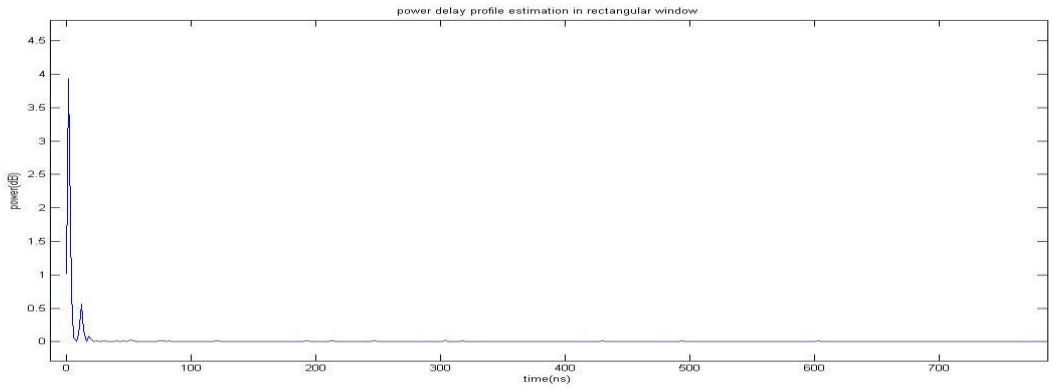


Figure 3.13 LOS Power Delay Profile using rectangular window

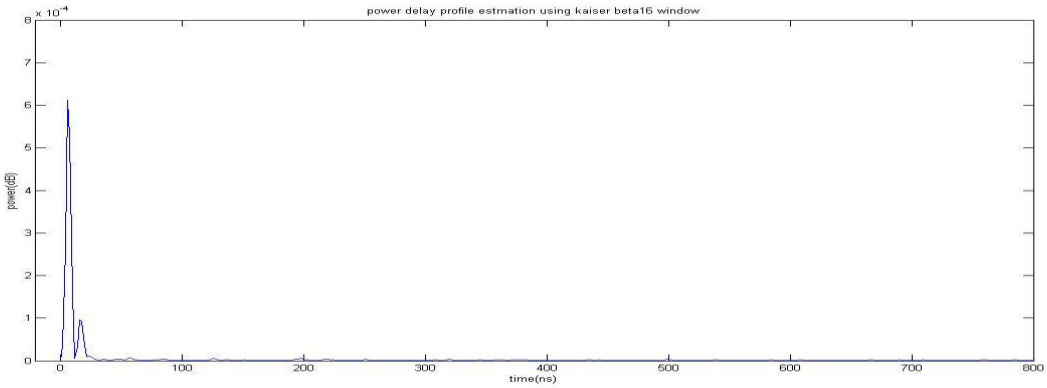


Figure 3.14 LOS Power Delay Profile using Kaiser Beta16 window

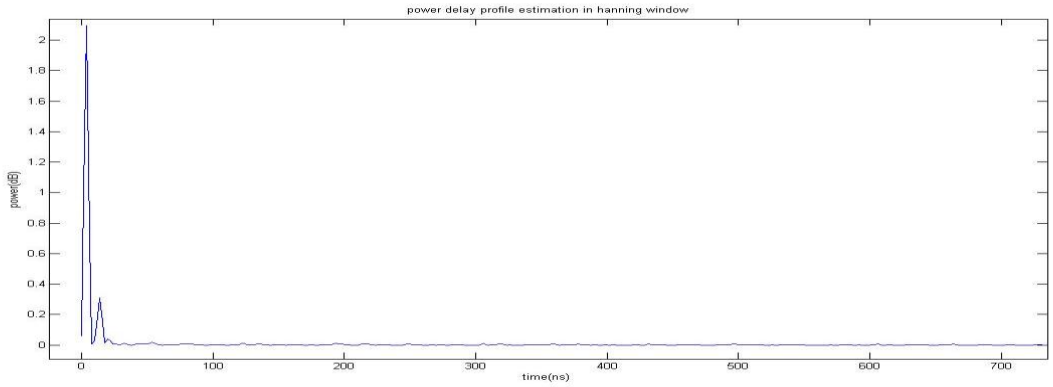


Figure 3.15 LOS Power Delay Profile using hanning window

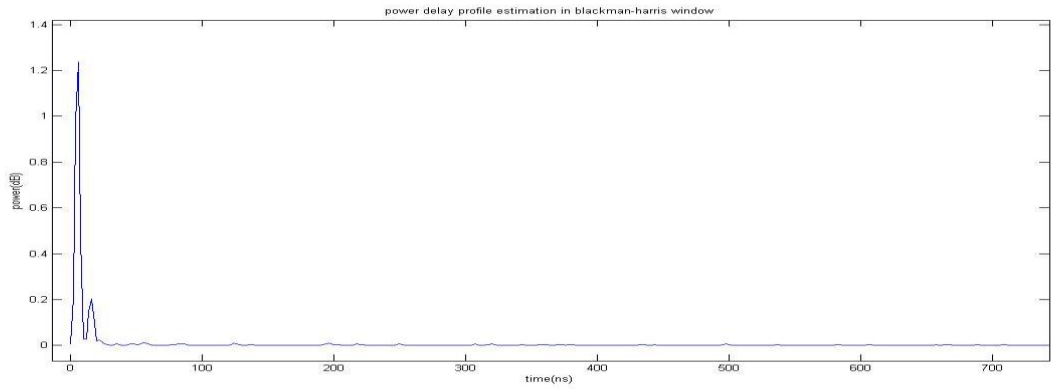


Figure 3.16 LOS Power Delay Profile using blackman-harris window

## *4.2 Processing of none line of sight propagation (NLOS) results*

We use the same signal, the same method to achieve transfer function $|H(j\omega)|$ of none light of sight results, to follow the same steps:

*Step 1: Truncation of different windows with* $|H(j\omega)|$

The frequency spectrum $|H(j\omega)|$ is truncated by different windows are shown in figure 4.1 to 4.4, respectively.

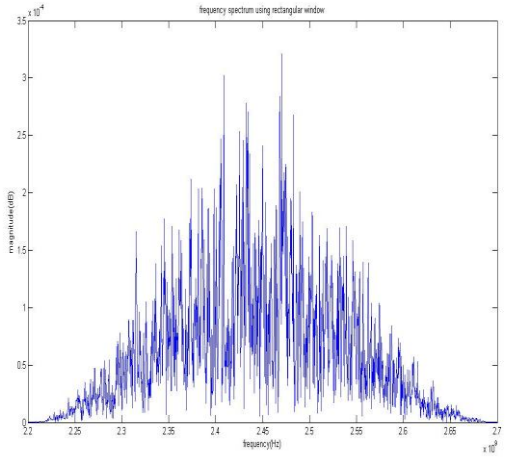


Figure 4.1 NLOS frequency spectrum using rectangular window

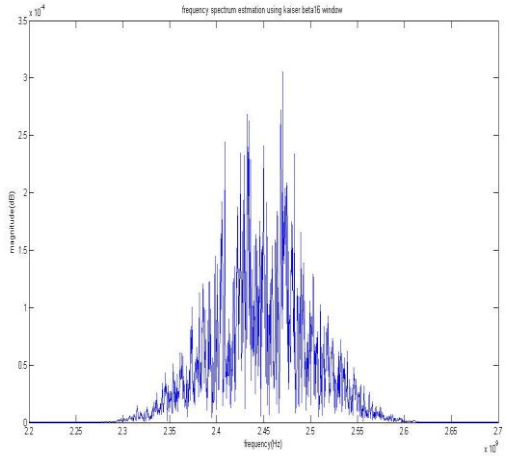


Figure 4.2 NLOS frequency spectrum using kaiser beta16 window

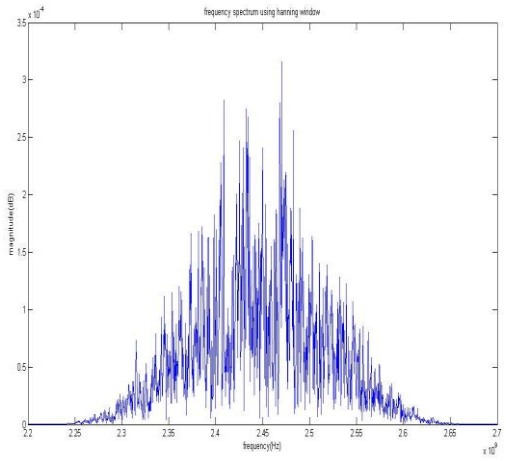


Figure 4.3 NLOS frequency spectrum using hanning window

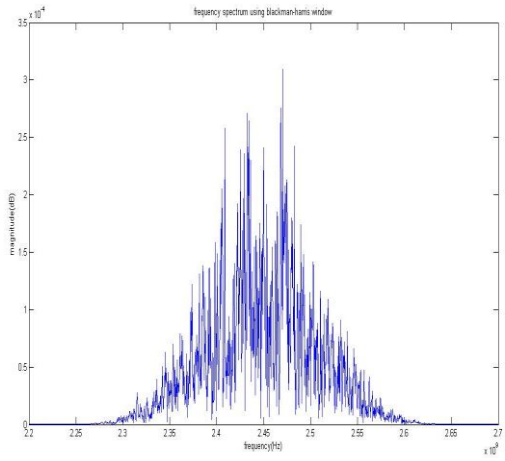


Figure 4.4 NLOS frequency spectrum using blackman-harris window

*Step 2 Phase angle estimation by applying hilbert transform*

The phase angle $\arg H(j\omega)$ is truncated by different windows are shown in figure 4.5 to 4.8, respectively.

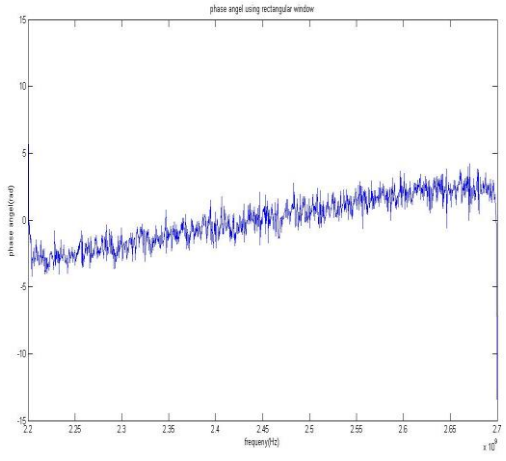


Figure 4.5 NLOS phase angle using rectangular window

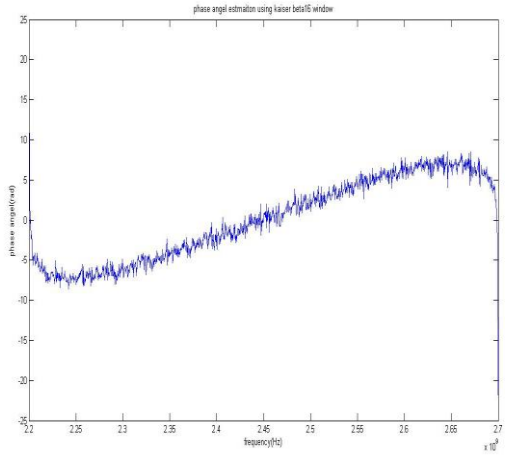


Figure 4.6 NLOS phase angle using kaiser beta16 window

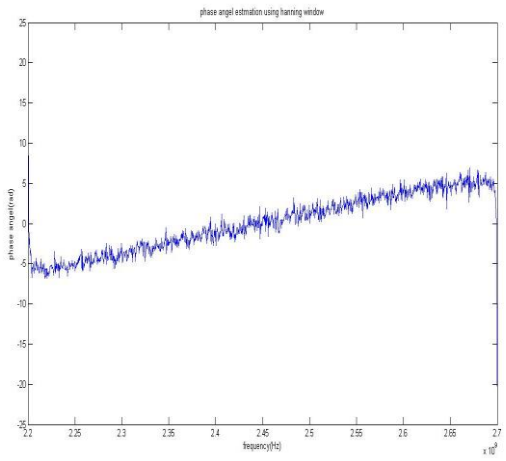

Figure 4.7 NLOS phase angle using rectangular window

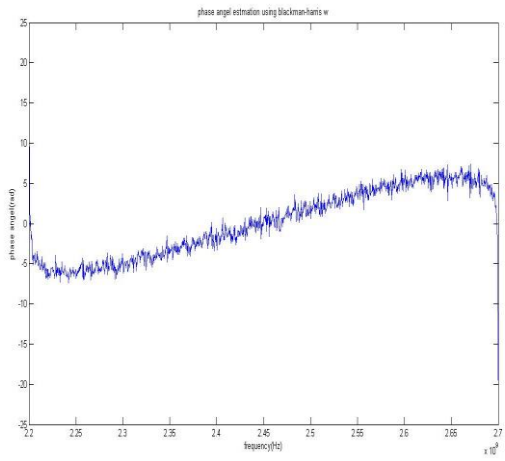

Figure 4.8 NLOS phase angle using blackman-harris window

*Step 3 Transform back to time-domain to obtain impulse response*

The figures 4.9 to 4.12 show the impulse response in rectangular window, Kaiser Beta16 window, hanning window, blackman-harris window:

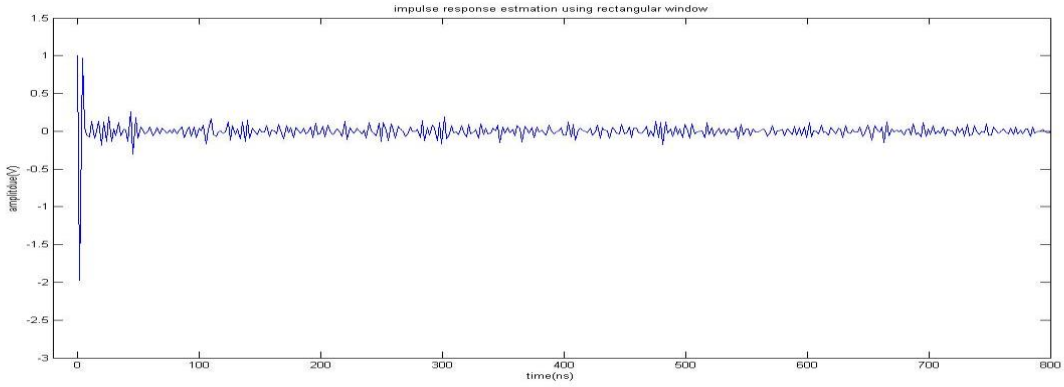


Figure 4.9 NLOS impulse response using rectangular window

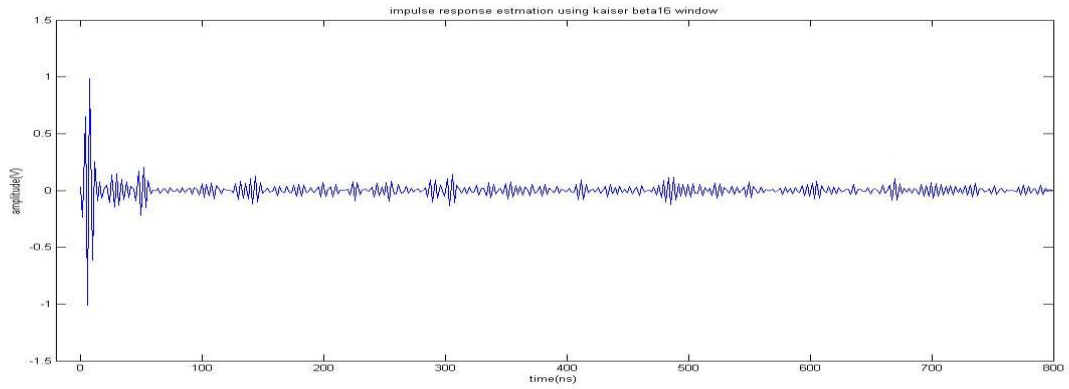


Figure 4.10 NLOS impulse response using Kaiser Beta16 window

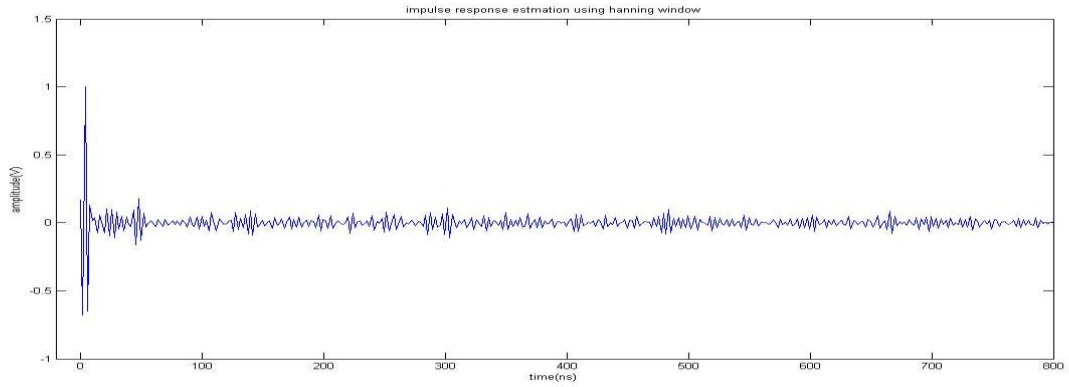


Figure 4.11 NLOS impulse response using hanning window

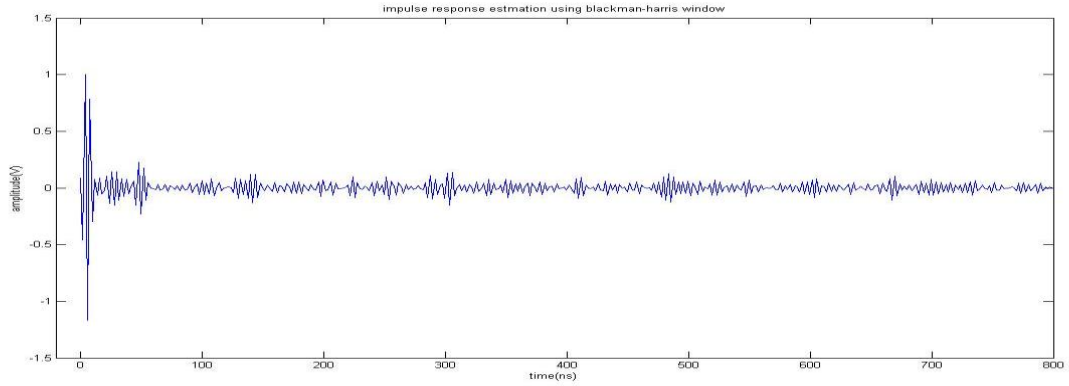


Figure 4.12 NLOS impulse response using blackman-harris window

*Step 4. Calculate power delay profile from impulse response*

Show PDP truncated in different window functions from figure 4.13 to 4.16:

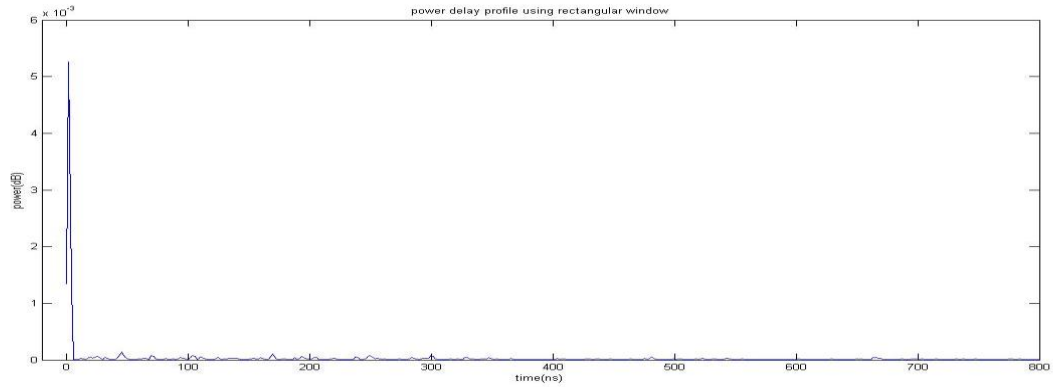


Figure 4.13 NLOS Power Delay Profile using rectangular window

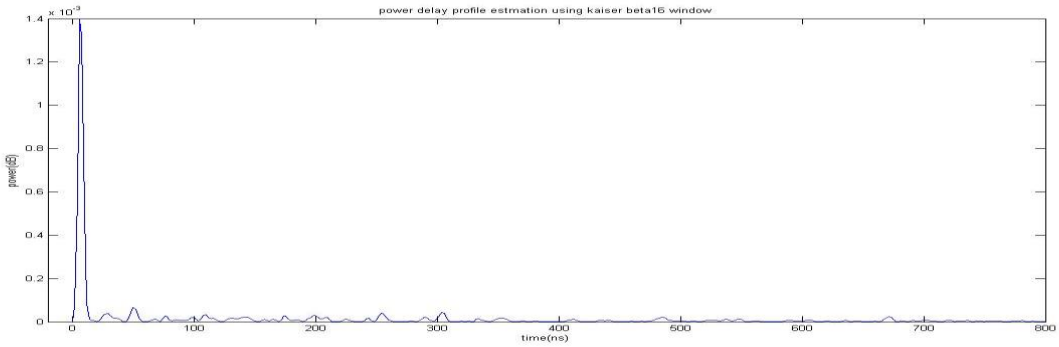


Figure 4.14 NLOS Power Delay Profile using Kaiser Beta16 window

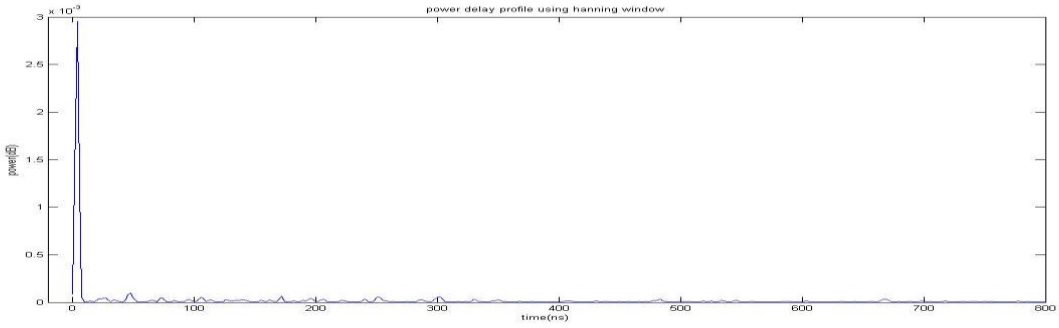


Figure 4.15 NLOS Power Delay Profile using hanning window

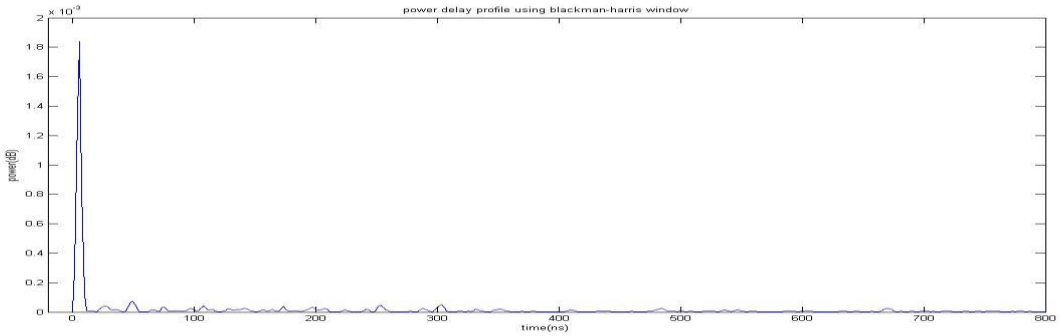


Figure 4.16 NLOS Power Delay Profile using blackman-harris window

Calculation and Comparison of mean delay and rms delay values between LOS and NLOS Propagation:

Follow the formula of the mean delay spread and rms delay spread:

Use $u = \frac{\sum_{n=1}^{M} nP(t)}{\sum_{n=1}^{M} P(t)}$ and $\sigma_{RMS} = \sqrt{\frac{\sum_{n=1}^{M} (n-u)^2 P(t)}{\sum_{n=1}^{M} P(t)}}$

Table of delay are shown below, table 2 shows the feature of light of sight propagation delay while table 3 shows non-light of sight propagation delay:

| | The delay spread for indoor channel, the distance is approximately 16m using line of sight propagation (LOS). | | | |
|---|---|---|---|---|
| Window Function | Rectangular | Kaiser Beta16 | Hanning | Blackman-Harris |
| Mean Delay Spread | 103.1014ns | 126.6271ns | 113.0781ns | 121.4628ns |
| RMS Delay Spread | 236.6814ns | 263.5867ns | 243.4372ns | 258.1574ns |

Table 2

| | The delay spread for indoor channel, the distance is approximately 16m using none line of sight propagation (NLOS). | | | |
|---|---|---|---|---|
| Window Function | Rectangular | Kaiser Beta16 | Hanning | Blackman-Harris |
| Mean Delay Spread | 140.8432ns | 154.2709ns | 146.8193ns | 151.7326ns |
| RMS Delay Spread | 244.8479ns | 257.6774ns | 250.6178ns | 255.4058ns |

Table 3

Conclusion for the LOS and NLOS delay spread:

Do the comparison on delay spread between light of sight and none light of sight propagation, mean delay of NLOS is normally

# 5. Discussion and Conclusion

For the phase estimation using SNA, in first illustration section we tried Kaiser Window with beta=2, which is more close to rectangular, a high resolution window, it has been found out in the simulation steps that the Blackman-Harris has the best performance among those 4 window functions, so In our experiment processing we use Kaiser window (with beta= 16), this window function has even lower resolution than Blackman-Harris, it is expected that it has a better output.

So in our experiment we apply in different window functions, high resolution window function: rectangular window, low resolution window function: Blackman-Harris, and Kaiser (β=16), where the Hanning window is modest window in between.

When we observe our phase estimation results, the higher resolution window contains low offset, which is different from the low resolution windows, have obvious offset like a ramp, it is because only the low resolution window functions have a suppression to the side band frequency, that's what we observed from the spectrum truncation, which the causality of the signal will be changed from this.

When the impulse responses are highlighted we can notice the impulse response from rectangular window is not distinct, while the ones under Blackman-Harris window and Kaiser (β=16) are much distinct and detectable, and Hanning window effect is in the between. The

same observation can be made to the power delay profile, the reason for these is rectangular window function does nothing but just cut the signal out of section, it will contain a lot spectrum leakage when signal goes from time domain to frequency domain, as well as lead the time domain leakage when signal goes from the frequency domain to the time. Generally speaking, NLOS impulse response will reveal that more and longer multi-paths are on the reflection ways, while in contrast LOS impulse response attenuated faster due to it has the shortest way to propagate.

Question will arise if we can use the window with the lower resolution even than Kaiser (β=16)? But if we use the low resolution window though we have low side lobe advantage, but we will have larger width of main lobe, that means the signal goes from frequency domain to time domain will not be accurate in the time, we cannot be exactly sure about what time the signal happens.

Both time domain leakage and the accuracy about the time, will be improved by increase the sampling frequency, see the result compare to the illustration former has 1601 point time resolution is about 2ns while latter has 201 points time resolution is about 9 μs, the results of higher resolution in different window have no much differences.

For Mean delay and rms delay, there are not much differences between windows either in light of sight or non-light of sight propagation, the trend is both in light of sight and Non-light of sight measurements, lower resolution window has bigger both mean delay and rms delay, higher resolution has shorter delay time. On the other hand, we observed that Non-light of sight propagation delay is greater than the light of sight propagation delay in respect of four types of different windows, exceptions are on the low resolution window, while the mean delay values follow the rules but for rms delay, NLOS values are less than the LOS rms values.

To use SNA instead of VNA to estimate light of sight and non-light of sight signals is based on Hilbert transform over the logarithm (base on mathematic constant e) of spectrum:
$\arg H(j\omega) = \Psi[\log|H(j\omega)|]$.

Impulse response h(t) is achieved from the transfer function H(jω) with its complex format. Power delay profile and rms delay is therefore obtained. The goal of research has been reached. For the mean delay and rms delay,

It is recommended to choose the lower resolution window to truncate with the detected spectrum before the phase estimation. The impulse response will be better amplitude accuracy due to less time domain leakage and suppression to the noise band of non-interest. In the work we choose Kaiser β=16 as the best window choice to do the measurements. It appears better responses.

We measured the RMS delay of indoor channel includes both LOS and NLOS propagation. Signals are truncated in different windows due to improve the accuracy of the results. Phase

angle is obtained by Hilbert Transform. Impulse Response is achieved by using inverse discrete fourier transform. In this method mean delay and rms delay can be found out. Our aims are fulfilled.

# 6. Acknowledgement

The Authors, Lai Jingou, Liu Che would like to appreciate Jóse Chilo, as a kind mentor provide laboratory room and instructions, Javier Ferrer Coll provide the instruments, Per Landin who gives us helps and advises in signal processing.

# 7. Reference

[1] Rytting, D., "ARFTG 50 year network analyzer history", in *Microwave Symp. Dig., IEEE MTT-S Int.,* Atlanta, GA, 2008, pp.11-18.[10.1109/MWSYM.2008.4633319].

[2] A. Bayram et al., "Frequency-domain measurement of indoor uwb channels," *Microwave and optical technology* Lett., pp. 118–123, JAN. 2005.[10.1002/mop.20563]

[3] A. Muqaibel, A. Safaai-Jazi, A. Attiya, B. Woerner, and S. Riad, "Path-Loss and Time Dispersion Parameters for Indoor UWB Propagation," *in IEEE trans. on wireless commun.*, vol. 5, NO. 3, pp. 550-559, MAR. 2006 [10.1109/TWC.2006.1611085]

[4] M. Z. Win, R. A. Scholtz, "Characterization of Ultra-Wide Bandwidth Wireless Indoor Channels: A Communication-Theoretic View" in *IEEE J. ON SELECTED AREAS IN COMMUN*., VOL. 20, NO. 9, pp. 1613-1627, DEC. 2002. [10.1109/JSAC.2002.805031]

[5] B. P. Donaldson et al., "Characterization of In-building UHF Wireless Communication channels using Spectral Energy Measurements", in *IEEE TRANS. ON ANTENNA AND PROPAGATION*, VOL. 44, NO.1, pp.80-86, JAN. 1996. [10.1109/8.477531]

[6] A.M.Street, L.Lukama, D.J.Edwards, ''Use of VNAs for wideband propagation measurements", in *Proc. Inst. Elect. Eng*., Vol. 148, pt. I, No. 6, pp. 411-415, Dec.2001. [10.1049/ip-com:20010639]

[7] H. Li et al., "Channel order and RMS delay spread estimation with application to AC power line communications" *Digital Signal Processing 13 (2003),* pp.284–300

[8] A. Muqaibel, A. Safaai-Jazi, B. Woerner, and S. Riad, "UWB Channel Impulse Response Characterization Using Deconvolution Techniques," *45th Midwest Symp. on Circuits and Systems*, vol. 3, pp. 605-608, 2002. [10.1109/MWSCAS.2002.1187112]

[9]Agrez, D., "Improving phase estimation with leakage minimization" in *Proc. of the 21st IEEE on Instrumentation and Measurement Technology Conference*, Vol. 1, pp. 162 – 167, May 2004. [10.1109/IMTC.2004.1351019]

[10] J. G. Proakis, D. G. Manolakis, *Digital Signal Processing,* 4th Edition, Upper Saddle River, NJ, 2007, ch.4, pp. 416-419

[11] Agilent Technology, *Agilent Time Domain Analysis Using a Network Analyzer Application Note 1287-12*, Agilent Technologies, Inc., March 9, 2007, literature number :5989-5723EN

[12] Jeffrey S. Beasley, Gary M., *Modern Electronic Communication,* 9th Edition, Pearson Prentice Hall, ch.12, pp.568-569,2008.

[13] G. E. Bottomley et al*.,* "A Generalized RAKE Receiver for Interference Suppression"*in IEEE J. ON SELECTED AREAS IN COMMUN.*, VOL. 18, NO. 8, AUG. 2000, [10.1109/49.864017]

# Appendix

## *Appendix A*

Comparison of 5 window functions:

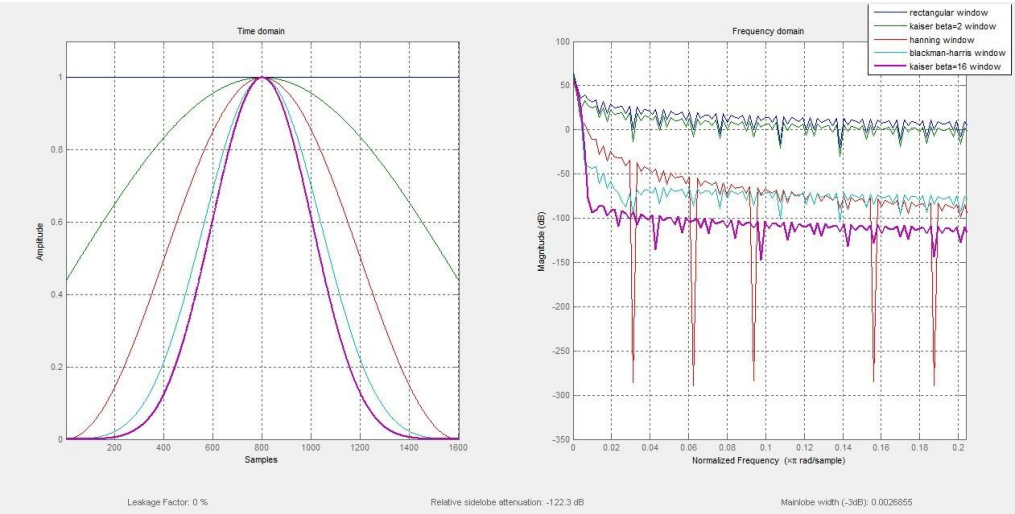


## *Appendix B*

Instruments information

<u>Function Generator HP 33120A:</u>

Useful Functionality:

To generate different types of signal with different frequency from 0.1Hz up to 15MHz, feed different amplitude into the external input port of Marconi Instruments 2031 10 kHz to 2700 MHz Signal Generator to modulate the RF signal.

Useful information:

Amplitude range:  50m~10Vpp

<u>Scalar Network Analyzer (HP 8757B)</u>

Useful Functionality:

Self-Test, test for the instrument functions well.

RF in port for fed the input RF signal.

Plug for detector, HP 85025, signal can be detected.

Connect DUT to attenuated output.

Attenuator HP8492A 10 dB can be attached used for amplification.

Input channel select for [CHANNEL 1] and [CHANNEL2] functions.

[Scale] function select for different resolution, [Auto scale] function can be selected for the instrument detection resolution.

[CURSOR] bottom is used for measurement reference line.

[PRESET] bottom for set configure in default condition.

Instruments information of implementation

Marconi Instruments 2031 10 kHz to 2700 MHz Signal Generator:

Useful Functionality:

Carrier signal frequency: 10 kHz to 2700 MHz

RF level: -144dBm to 13dBm

Modulate RF signal (AM) with different depth used source in fed by a Function Generator (HP 33120A).

## *Appendix C*

Matlab command

Windowing truncation

```
Y_rect=Y.*rectwin(1601)';   % rectwin could be changed to kaiser(1601,2), kaiser(1601,16), hann(1601), blackmanharris(1601).

X_rect=X.*rectwin(1601)';   % the same as above.
```

Vector division

```
H=Y./X;        % X,Y,H are same dimension vectors
```

Phase estimation

```
H_log=log(H);
```

```
H_phase=imag(hilbert(H_log));    % two steps to get phase angle

Complex vector

Hjw=H.*(cos(H_phase)+i*sin(H_phase));

Impulse response

ht=czt(Hjw);   % ht returns to be a same dimension vector as Hjw.

Power delay profile

Pt=abs(ht).*abs(ht);

Mean delay

n=1:1601;

u=(Pt*n)/sum(Pt);

RMS delay

rms=((Pt*((n-u).*(n-u)))/sum(Pt))^(0.5);

Figure plotting

t=0:1/(0.5/1600*1601):1/(0.5/1600*1601)*1600;   % 1/(0.5/1600*1601) is the resolution of time

plot(t,ht);
```